DOI: 10.1002/anie.201205625

Amyloids

Solid-State NMR Spectroscopy of Functional Amyloid from a Fungal Hydrophobin: A Well-Ordered β-Sheet Core Amidst Structural Heterogeneity**

Vanessa K. Morris, Rasmus Linser, Karyn L. Wilde, Anthony P. Duff, Margaret Sunde, and Ann H. Kwan**

Class I hydrophobins are small amphipathic proteins that self-assemble to form functional amyloid fibrils, known as rodlets, on the surface of fungal structures such as aerial hyphae and spores. The rodlets form a monolayer through lateral association and are highly robust; dissociation is only possible with certain concentrated acids. This monolayer is amphipathic, with the hydrophobic face as water-resistant as Teflon.[1] In fungal biology the layer serves a number of important roles, including conferring water resistance to spores and mediating fungus–host interactions.

Structural information on hydrophobins is critical for understanding the molecular interactions that define the rodlet assembly process and to aid the design of both antifungal agents and novel hydrophobin-based nanomaterials. EAS is a class I hydrophobin from *Neurospora crassa* and is so named because mutants lacking this protein displayed an easily wettable (EAS) phenotype.[2] The structures of the soluble form of EAS and a functional truncated variant, $EAS_{\Delta 15}$, have been determined by solution NMR spectroscopy. The structures display the β-sheet topology unique to hydrophobins (Figure 1 A).[3] The surface exhibits a clear separation of charged and hydrophobic amino acid residues that makes the proteins highly amphipathic and surface-active (Figure 1 B). Recombinantly produced EAS and $EAS_{\Delta 15}$ spontaneously assemble into rodlet monolayers at hydrophobic–hydrophilic interfaces with the same regular, well-packed morphology as is observed on fungal structures and the same ability to reverse the wettability of surfaces (Figure 1 C,D). Circular dichroism (CD) spectra indicate that the assembled rodlets are rich in β-sheet structure, while soluble $EAS_{\Delta 15}$ shows little regular secondary structure (Figure 1 E).[3] Detailed structural information from the assembled rodlet monolayers has so far proved elusive owing to their inherently insoluble and non-crystalline nature.

Magic-angle-spinning (MAS) solid-state NMR (ssNMR) has become the primary method for yielding detailed structural information on fibrillar proteins,[4] and in favorable cases multiple conformations can be distinguished.[5] In general, only local order is required to yield ssNMR spectra of sufficient quality for structural information to be derived. Recent advances, including ^{1}H-detected heteronuclear experiments, have made possible ssNMR structure determination and dynamics studies of well-ordered systems, such as microcrystalline proteins[6] and ordered amyloid fibrils.[4c,d,7] These methods add an additional nucleus as a source of information and greatly enhance spectroscopic possibilities.[8]

Solid-state NMR spectra of the functional $EAS_{\Delta 15}$ rodlets were obtained on double- and triple-labeled $EAS_{\Delta 15}$ rodlet samples. The $EAS_{\Delta 15}$ spectra generally show broad NMR signals indicative of conformational heterogeneity. However, despite the overall broadness of the signals, both proton-detected $^{15}N/^{1}H$ correlations from sparsely protonated samples as well as $^{13}C/^{13}C$ correlation spectra recorded on protonated rodlets show that a subset of the resonances are notably well defined. Figure 1 G shows the solid-state $^{15}N/^{1}H$ correlation spectrum of deuterated and partly ^{1}H-back-exchanged rodlets. Highly indicative of the hydrogen-bonding network, $^{15}N/^{1}H$ correlations are commonly used for charac-

[*] V. K. Morris,[+] M. Sunde, A. H. Kwan
School of Medical Sciences and School of Molecular Bioscience, University of Sydney
Sydney (Australia)
E-mail: ann.kwan@sydney.edu.au
margaret.sunde@sydney.edu.au
R. Linser[+]
School of Chemistry, University of New South Wales
Sydney (Australia)
R. Linser[+]
Department of Biological Chemistry and Molecular Pharmacology, Harvard Medical School
Boston (USA)
K. L. Wilde, A. P. Duff
National Deuteration Facility, Australian Nuclear Science and Technology Organisation
Lucas Heights (Australia)
[+] These authors contributed equally to this work.

[**] We thank Dr. J. Hook, Dr. D. Thomas, and Dr. D. Lawes from the NMR facility at University of New South Wales for spectrometer access and assistance, Dr. N. Shepherd and Dr. B. Crossett for mass spectrometry at the Sydney University Proteome Research Unit, and Dr. A. Kondyurin for assistance with contact angle measurements. The authors acknowledge the facilities, and the scientific and technical assistance, of the Australian Microscopy & Microanalysis Research Facility at the Electron Microscope Unit, University of Sydney. The HET-s spectrum was kindly provided by Dr. C. Wasmer and Prof. B. Meier. The project was funded by the Australian Research Council (LP0776672 and DP0879121) and ANSTO Bragg Institute (NDF 1668). M.S. was supported by a National Health and Medical Research Council R.D. Wright Career Development Fellowship, V.K.M. was supported by a University of Sydney Vice-Chancellor's Research Scholarship, and R.L. was supported by an Australian Research Council Discovery Early Career Research Award.

Supporting information for this article is available on the WWW under http://dx.doi.org/10.1002/anie.201205625.

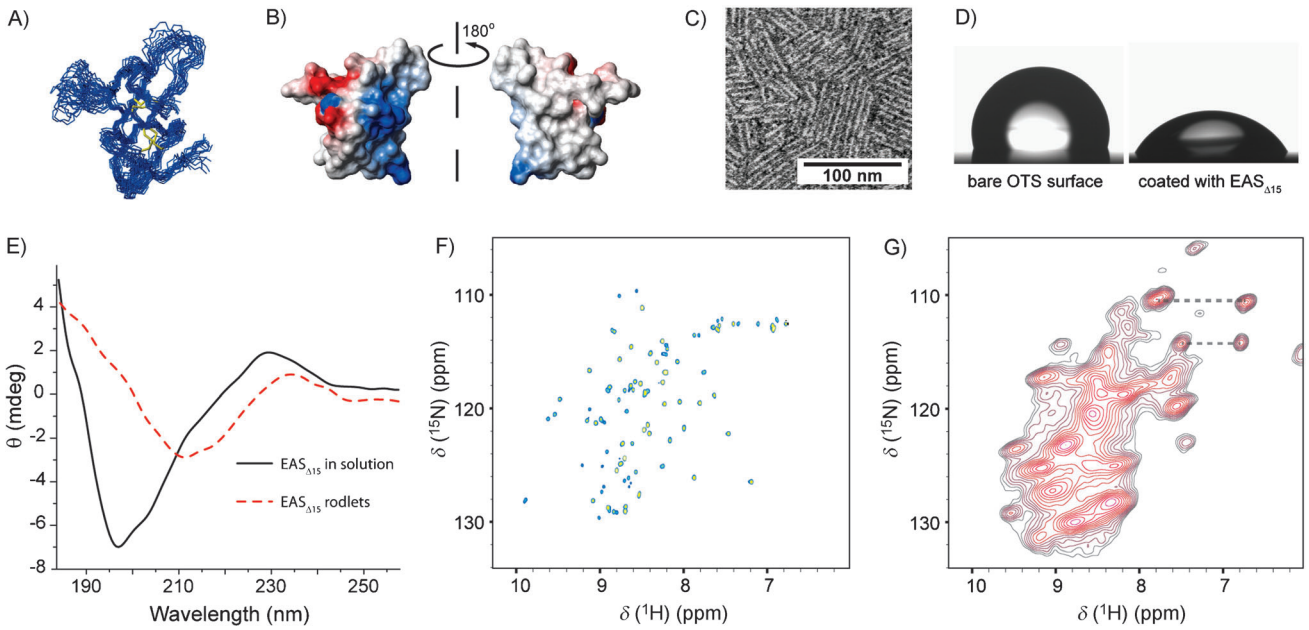

Figure 1. Comparison of solution-state (monomer) and solid-state (rodlet) properties of hydrophobin EAS$_{\Delta15}$. A) Overlay of the 20 lowest energy structures of monomeric EAS$_{\Delta15}$ (PDB code 2k6a). B) Electrostatic surface of monomeric EAS$_{\Delta15}$. C) Negatively stained transmission electron micrograph of EAS$_{\Delta15}$ rodlets. D) Water droplets on bare octadecyltrichlorosilane (OTS)-treated silicon wafer and on EAS$_{\Delta15}$-coated OTS-treated silicon wafer layer. E) CD spectra of EAS$_{\Delta15}$ in water and as rodlets dried onto a quartz cuvette. Experimental details are available in the Supporting Information. F) ^{15}N/^{1}H-HSQC spectrum recorded on monomeric EAS$_{\Delta15}$ in solution. G) ^{1}H-detected solid-state ^{15}N/^{1}H correlation of EAS rodlets under comparable buffer conditions as in (F). Dashed lines indicate peaks that arise from side-chain amides.

terization of the protein fold in solution-state NMR spectroscopy. This approach could be transferred to the solid state in a straightforward manner, largely facilitated by partly ^{1}H-back-substituted ^{2}H,^{13}C,^{15}N-labeled protein samples. In the ^{15}N/^{1}H correlation spectrum recorded on EAS rodlets, a subset of resonances stand out against a broad and poorly defined bulk; they can be further distinguished by apodization or ^{1}H T_1-modulated representation (Supporting Information, Figure S4). These observations suggest that the EAS$_{\Delta15}$ rodlets have a twofold molecular composition, with a structurally conserved and tightly packed core among a heterogeneous ensemble of conformationally disordered regions.

A direct comparison of ^{15}N/^{1}H correlations recorded from rodlets in the solid state with corresponding spectra from the monomer reveals that the pattern obtained from the structurally conserved amino acid residues in the rodlets deviates significantly from that obtained from the monomer in solution (Figure 1 F,G; see the Supporting Information, Figure S5 for an overlay). The solid-state spectrum also includes new signals from ordered Gln or Asn amide side chains, two amino acid residue types which have been implicated in forming intermolecular side-chain ladder interactions in other amyloid structures.[9] These changes are in marked contrast to the behavior of proteins that maintain their fold upon precipitation,[10] and reveal a substantial structural rearrangement upon EAS$_{\Delta15}$ fibril formation. For many of the distinct and intense peaks found only in the rodlet spectra, both local mobility (as outlined by ^{1}H T_1 data and ^{15}N/^{1}H correlations comparing dipolar and scalar magnetization transfers) as well as peak positions support the formation of new structured elements in the rodlets (Supporting Information, Figure S1 C, S4, and S5). Incomplete proton back-substitution into exchangeable positions has been excluded by H/D exchange experiments.

We were not able to obtain any sequential assignments using HNCA/HNCO[7] and hCxhNH[12] (on partially ^{1}H-back-exchanged deuterated samples) or NCACX/NCOCX[6a] experiments (on protonated samples) owing to the overall low definition of the spectra and low signal-to-noise ratios. Instead, MAS ^{13}C/^{13}C correlation spectra under various mixing schemes were recorded on protonated EAS$_{\Delta15}$ samples (Figure 2; Supporting Information, Figures S2 and S3). These were compared to previous solid-state NMR studies of other protein fibrils. The substantial structural heterogeneity observed in the EAS$_{\Delta15}$ rodlet spectrum (Figure 2 B), as evident from the broadness of most signals, is similar to that observed for full-length HET-s fibrils[13] but in contrast to the very well-defined and clearly resolved spectra observed for ordered fibrils. The latter include fibrils of HET-s (218–289),[4c] which has a similar monomer size to EAS$_{\Delta15}$ (Figure 2 C), fibrils of an 11-residue amyloidogenic peptide derived from transthyretin[4a] or fibrils formed by the 40-residue Aβ peptide.[4d] Although fibrils composed of higher-molecular-weight proteins can also yield well-resolved spectra,[14] it is notable that the higher quality solid-state NMR spectra were mostly recorded on amyloid structures formed from shorter peptides or the isolated amyloidogenic region only, whereas the whole functional EAS$_{\Delta15}$ protein unit is present in the rodlets examined here. The structural disorder observed on the molecular scale in the EAS$_{\Delta15}$ rodlets is in contrast to the apparent order on the supramolecular scale, as

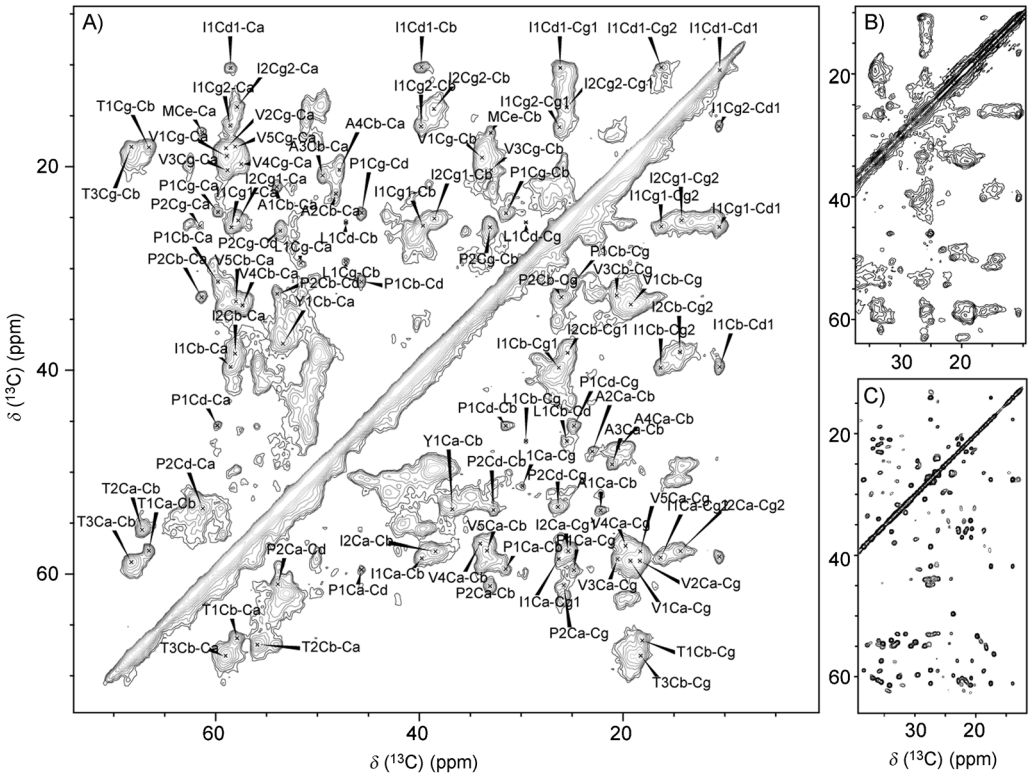

Figure 2. The inherent structural heterogeneity of $EAS_{\Delta15}$ rodlets reflected in ^{13}C homonuclear correlations. A) $^{13}C/^{13}C$ correlation spectrum of $EAS_{\Delta15}$ showing intraresidue correlations. The numbers denote that the peaks belong to the same spin system. B,C) Comparison between (B) a rodlet preparation of the hydrophobin $EAS_{\Delta15}$ (B) and prion fibrils (C, courtesy of Prof. Beat Meier) prepared from fungal HET-s (218–289).[4c] See the Supporting Information, Figures S2 and S3 for spectra recorded with different mixing times/schemes as well as for a comparison with rodlets formed by DewA, another rodlet-forming hydrophobin.[11]

evidenced by the consistently well-packed and regular morphology of the rodlets as imaged by atomic force microscopy and electron microscopy on a range of substrates.[2]

Despite the apparent disorder, resolved resonance sets from about 18 amino acid residues could be identified, which were mostly Ala, Ile, Thr, Val, and Pro. Figure 2A shows annotations corresponding to amino acid types identified with the help of $^{13}C/^{13}C$ homonuclear correlation spectroscopy using DARR mixing and a 3D NCACX experiment. The two cross-peaks at a chemical shift of $\delta = 50$ ppm/15 ppm may have arisen from Ala residues with upfield-shifted Cβ atoms or, despite their presence in the short mixing time (5 ms) PDSD spectra, may represent very close inter-residue contacts. Unresolved cross-peaks in the region around $\delta = 35$–40 ppm/50–55 ppm probably correspond to Cα/Cβ contacts from Cys, Asp, and Asn residues.

Chemical shifts in the $^{15}N/^{1}H$ correlation spectra directly reflect the underlying secondary structure. These correlations from ^{1}H-back-exchanged triple-labeled $EAS_{\Delta15}$ rodlets are generally shifted downfield and represent a typical β-sheet distribution. For the $^{13}C/^{13}C$ correlations, secondary chemical shifts (ΔCα-ΔCβ) were generated and compared to their random coil analogues.[15] In analogy to a chemical shift index, consideration of the Cα and Cβ values extracted for single amino acid residues suggests a β-sheet conformation in the majority of cases (Figure 3). Although five Val Cγ peaks could be assigned, the Cβ peaks were more overlapped; thus only two Val residues were included in the secondary chemical-shift analysis. However, the other three Val residues would be expected to have similar secondary chemical shifts and are likely to be in a β-sheet conformation.

As with other amyloid structures, non-residue-specific spectroscopic methods such as CD spectropolarimetry, Fourier transform infrared spectroscopy, and X-ray fiber diffraction indicate that an intermolecular β-sheet motif connects $EAS_{\Delta15}$ monomers within the rodlet structure.[18] To form intermolecular β-sheets, either pre-existing β-strands in the $EAS_{\Delta15}$ monomer structure must pack against those from a neighboring monomer, or a structural rearrangement revealing new β-strands capable of forming intermolecular hydrogen bonds must occur. Such structural changes have been observed for a number of other amyloid fibrils, such as the Aβ fibrils associated with Alzheimer's disease.[19] The region of EAS postulated to form the cross-β core upon rodlet formation has been localized in the primary sequence.[17] Our solid-state NMR data give direct experimental evidence for substantial structural changes in the monomer and formation of new secondary structural elements within the rodlets, consistent with the hypothetical model constructed from functional assays and mutagenesis data.[18] Furthermore, the disorder observed in the solid-state NMR spectra is consistent

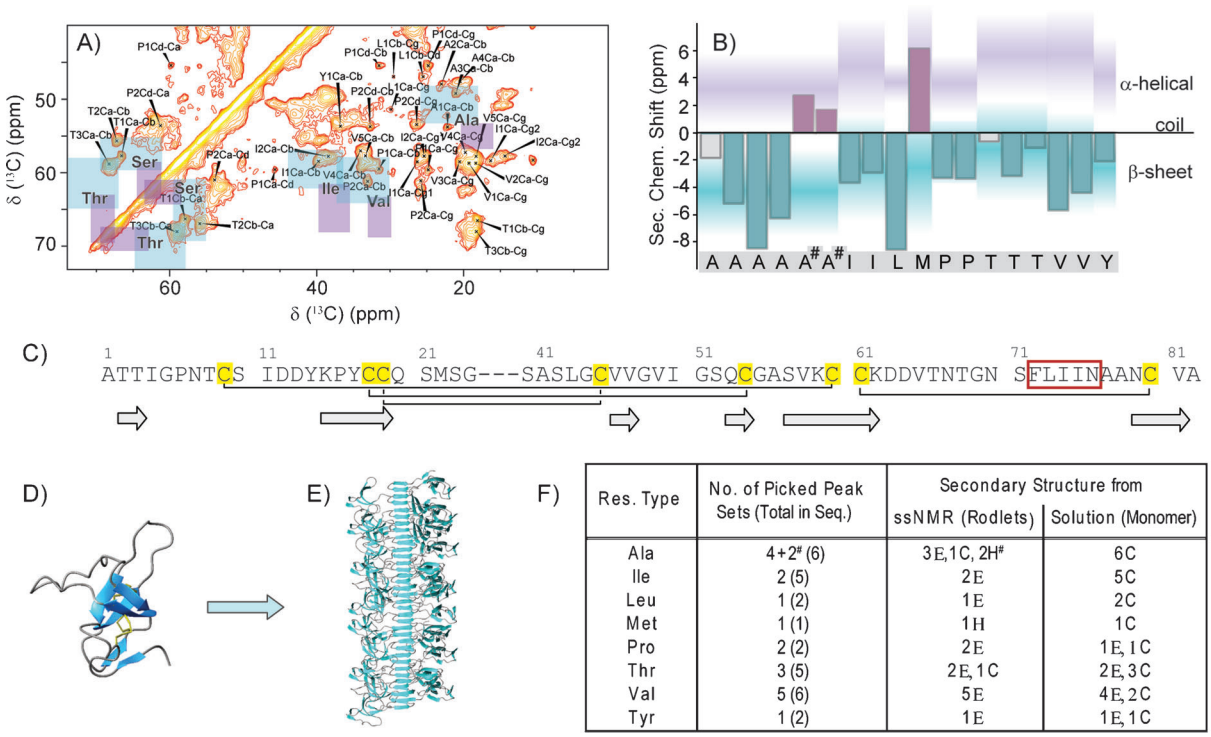

Res. Type	No. of Picked Peak Sets (Total in Seq.)	Secondary Structure from ssNMR (Rodlets)	Secondary Structure from Solution (Monomer)
Ala	4+2# (6)	3E,1C, 2H#	6C
Ile	2 (5)	2E	5C
Leu	1 (2)	1E	2C
Met	1 (1)	1H	1C
Pro	2 (2)	2E	1E, 1C
Thr	3 (5)	2E, 1C	2E, 3C
Val	5 (6)	5E	4E, 2C
Tyr	1 (2)	1E	1E, 1C

Figure 3. Secondary chemical shifts for amino acid-type assigned residues in $EAS_{\Delta15}$. A) Most $EAS_{\Delta15}$ chemical shifts fall into β-sheet regions (cyan) rather than showing random-coil or α-helical shifts (purple) in the $^{13}C,^{13}C$ correlation spectrum.[16] The colored regions represent two standard deviations (σ) from the average of the chemical shifts associated with the secondary structure. B) ΔCα-ΔCβ values (denoted secondary chemical shift) of the amino acid residues that could be identified. Purple and cyan shades represent expected values of ΔCα-ΔCβ for α-helical and β-sheet residues,[16] respectively, with the most intense band marking the average values and the shades fading out at ±σ from the mean. The bar corresponding to the secondary chemical shift for each amino acid residue is colored in purple, cyan, or gray according to the classification as α-helical, β-sheet, or random coil structures, respectively. # marks the two amino acid residues which have been tentatively assigned as Ala based on cross-peaks at $\delta \sim 50$ ppm/15 ppm. C) Amino acid sequence of $EAS_{\Delta15}$ with cysteine residues highlighted in yellow. Numbering is according to the amino acid sequence in mature, full-length EAS. The secondary structure of $EAS_{\Delta15}$ in solution is given underneath, where arrows represent β-strands. Amino acid residues belonging to the amyloidogenic sequence as identified in a previous mutagenesis study[17] are boxed. D) Ribbon diagram of $EAS_{\Delta15}$ solution structure. E) Illustration of proposed rodlet model displaying cross-β structure assembled from multiple $EAS_{\Delta15}$ monomers after a simple conformational change.[17] F) Amino acid residues identified in the solid-state spectra and their probable secondary structure (based on literature values)[16] as compared with secondary structure observed in the monomer. β-sheet, α-helix, and coil are represented as E, H, and C, respectively.

with the putative rodlet model, where the cross-β core is well defined while the remainder of the structure in each monomer can be accommodated in many ways without affecting the lateral packing between individual rodlets or the overall amphipathicity of the monolayer.

This study uses the entire functional amyloid form rather than the fibril core only. Thus it is possible that the structural heterogeneity in the non-core regions is a native, inherent, and even required feature of the rodlet monolayers. Notably, all $^{15}N/^{1}H$ and $^{13}C/^{13}C$ correlations of $EAS_{\Delta15}$ rodlets were reproducible across different preparations and all presented ensemble distributions (Supporting Information, Figure S1 A). Structural heterogeneity may offer additional functionality, such as to allow the rodlets to pack into monolayers with tight lateral association (a feature not present in other amyloid fibrils)[17] or to coat surfaces with different geometries on the nanometer scale. A recent study of the functional amyloid Pmel17 has also demonstrated that conformational variation around a basic structural motif can give rise to the same biological function.[20]

Even though spectroscopic characterization is much more challenging for whole functional proteins with mixed structural characteristics than for truncated fragments with a homogeneous nature, the ability to characterize these systems and their molecular (sub)structures remains worthwhile and may reveal unique insights into biological functions. We have shown that hydrophobin rodlets are largely composed of a β-sheet structure that has a substantially altered protein fold compared to the monomer in solution. The structurally defined β-sheet core exists within a larger-scale architecture that exhibits structural heterogeneity but which is compatible with the formation of rodlets of regular morphology that associate into monolayers.

Received: July 16, 2012
Published online: November 4, 2012

Keywords: amyloids · fibrous proteins · hydrophobins · magic-angle spinning · solid-state NMR spectroscopy

[1] H. A. Wösten, M. L. de Vocht, *Biochim. Biophys. Acta Rev. Biomembr.* **2000**, *1469*, 79 – 86.

[2] M. Sunde, A. H. Kwan, M. D. Templeton, R. E. Beever, J. P. Mackay, *Micron* **2008**, *39*, 773 – 784.

[3] A. H. Kwan, I. Macindoe, P. V. Vukasin, V. K. Morris, I. Kass, R. Gupte, A. E. Mark, M. D. Templeton, J. P. Mackay, M. Sunde, *J. Mol. Biol.* **2008**, *382*, 708 – 720.

[4] a) C. P. Jaroniec, C. E. MacPhee, V. S. Bajaj, M. T. McMahon, C. M. Dobson, R. G. Griffin, *Proc. Natl. Acad. Sci. USA* **2004**, *101*, 711 – 716; b) A. K. Paravastu, R. D. Leapman, W. M. Yau, R. Tycko, *Proc. Natl. Acad. Sci. USA* **2008**, *105*, 18349 – 18354; c) C. Wasmer, A. Lange, H. v. Melckebeke, A. B. Siemer, R. Riek, B. H. Meier, *Science* **2008**, *319*, 1523 – 1526; d) J.-M. Lopez del Amo, M. Schmidt, U. Fink, M. Dasari, M. Fändrich, B. Reif, *Angew. Chem.* **2012**, *124*, 6240 – 6243; *Angew. Chem. Int. Ed.* **2012**, *51*, 6136 – 6139.

[5] J. T. Nielsen, M. Bjerring, M. D. Jeppesen, R. O. Pedersen, J. M. Pedersen, K. L. Hein, T. Vosegaard, T. Skrydstrup, D. E. Otzen, N. C. Nielsen, *Angew. Chem.* **2009**, *121*, 2152 – 2155; *Angew. Chem. Int. Ed.* **2009**, *48*, 2118 – 2121.

[6] a) F. Castellani, B.-J. van Rossum, A. Diehl, M. Schubert, K. Rehbein, H. Oschkinat, *Nature* **2002**, *420*, 98 – 102; b) M. J. Knight, A. L. Webber, A. J. Pell, P. Guerry, E. Barbet-Massin, I. Bertini, I. C. Felli, L. Gonnelli, R. Pierattelli, L. Emsley, T. Herrmann, G. Pintacuda, *Angew. Chem.* **2011**, *123*, 11901 – 11905; *Angew. Chem. Int. Ed.* **2011**, *50*, 11697 – 11701.

[7] R. Linser, M. Dasari, M. Hiller, V. Higman, U. Fink, J.-M. Lopez del Amo, S. Markovic, L. Handel, B. Kessler, P. Schmieder, D. Oesterhelt, H. Oschkinat, B. Reif, *Angew. Chem.* **2011**, *123*, 4601 – 4605; *Angew. Chem. Int. Ed.* **2011**, *50*, 4508 – 4512.

[8] a) R. Linser, U. Fink, B. Reif, *J. Magn. Reson.* **2008**, *193*, 89 – 93; b) R. Linser, B. Bardiaux, V. Higman, U. Fink, B. Reif, *J. Am. Chem. Soc.* **2011**, *133*, 5905 – 5912; c) P. Schanda, B. H. Meier, M. Ernst, *J. Am. Chem. Soc.* **2010**, *132*, 15957 – 15967.

[9] M. S. Dueholm, S. V. Petersen, M. Sonderkaer, P. Larsen, G. Christiansen, K. L. Hein, J. J. Enghild, J. L. Nielsen, K. L. Nielsen, P. H. Nielsen, D. E. Otzen, *Mol. Microbiol.* **2010**, *77*, 1009 – 1020.

[10] V. Chevelkov, Y. Xue, R. Linser, N. Skrynnikov, B. Reif, *J. Am. Chem. Soc.* **2010**, *132*, 5015 – 5017.

[11] M. A. Stringer, W. E. Timberlake, *Mol. Microbiol.* **1995**, *16*, 33 – 44.

[12] R. Linser, *J. Biomol. NMR* **2012**, *52*, 151 – 158.

[13] C. Wasmer, A. Schütz, A. Loquet, C. Buhtz, J. Greenwald, R. Riek, A. Böckmann, B. H. Meier, *J. Mol. Biol.* **2009**, *394*, 119 – 127.

[14] B. Habenstein, L. Bousset, Y. Sourigues, M. Kabani, A. Loquet, B. H. Meier, R. Melki, A. Böckmann, *Angew. Chem.* **2012**, *124*, 8087 – 8090; *Angew. Chem. Int. Ed.* **2012**, *51*, 7963 – 7966.

[15] D. S. Wishart, B. D. Sykes, *Meth. Enzymol.* **1994**, *239*, 363 – 392.

[16] Y. Wang, O. Jardetzky, *Protein Sci.* **2002**, *11*, 852 – 861.

[17] I. Macindoe, A. H. Kwan, Q. Ren, V. K. Morris, W. Yang, J. P. Mackay, M. Sunde, *Proc. Natl. Acad. Sci. USA* **2012**, *109*, E804 – E811.

[18] a) J. P. Mackay, J. M. Matthews, R. D. Winefield, L. G. Mackay, R. G. Haverkamp, M. D. Templeton, *Structure* **2001**, *9*, 83 – 91; b) A. H. Y. Kwan, R. D. Winefield, M. Sunde, J. M. Matthews, R. G. Haverkamp, M. D. Templeton, J. P. Mackay, *Proc. Natl. Acad. Sci. USA* **2006**, *103*, 3621 – 3626.

[19] a) M. Dasari, A. Espargaro, R. Sabate, J.-M. Lopez del Amo, U. Fink, G. Grelle, J. Bieschke, S. Ventura, B. Reif, *ChemBioChem* **2011**, *12*, 407 – 423; b) I. Bertini, L. Gonnelli, C. Luchinat, J. Mao, A. Nesi, *J. Am. Chem. Soc.* **2011**, *133*, 16013 – 16022.

[20] K. N. Hu, R. P. McGlinchey, R. B. Wickner, R. Tycko, *Biophys. J.* **2011**, *101*, 2242 – 2250.

